



Excess methane emissions from shallow water platforms elevate the carbon intensity of US Gulf of Mexico oil and gas production

Alan M. Gorchov Negron^{a,1} , Eric A. Kort^{a,1} , Yuanlei Chen^b , Adam R. Brandt^b , Mackenzie L. Smith^c , Genevieve Plant^a , Alana K. Ayasse^{d,e} , Stefan Schwietzke^f , Daniel Zavala-Araiza^f, Catherine Hausman^g, and Ángel F. Adames-Corraliza^h

Edited by Joost A. de Gouw, University of Colorado Boulder, Boulder, CO; received September 6, 2022; accepted February 17, 2023 by Editorial Board Member Akkihebbal R. Ravishankara

The Gulf of Mexico is the largest offshore fossil fuel production basin in the United States. Decisions on expanding production in the region legally depend on assessments of the climate impact of new growth. Here, we collect airborne observations and combine them with previous surveys and inventories to estimate the climate impact of current field operations. We evaluate all major on-site greenhouse gas emissions, carbon dioxide (CO₂) from combustion, and methane from losses and venting. Using these findings, we estimate the climate impact per unit of energy of produced oil and gas (the carbon intensity). We find high methane emissions (0.60 Tg/y [0.41 to 0.81, 95% confidence interval]) exceeding inventories. This elevates the average CI of the basin to 5.3 g CO₂e/MJ [4.1 to 6.7] (100-y horizon) over twice the inventories. The CI across the Gulf varies, with deep water production exhibiting a low CI dominated by combustion emissions (1.1 g CO₂e/MJ), while shallow federal and state waters exhibit an extraordinarily high CI (16 and 43 g CO₂e/MJ) primarily driven by methane emissions from central hub facilities (intermediaries for gathering and processing). This shows that production in shallow waters, as currently operated, has outsized climate impact. To mitigate these climate impacts, methane emissions in shallow waters must be addressed through efficient flaring instead of venting and repair, refurbishment, or abandonment of poorly maintained infrastructure. We demonstrate an approach to evaluate the CI of fossil fuel production using observations, considering all direct production emissions while allocating to all fossil products.

methane | carbon | intensity | gulf | production

The combustion of fossil fuels is the largest historical and contemporary anthropogenic source of greenhouse gases (1). In addition to consumer end use of fossil fuels, the production of fossil fuels emits substantial greenhouse gases through combustion processes releasing carbon dioxide (CO₂) and venting and losses of natural gas releasing methane (CH₄). Atmospheric observations in oil and gas basins can be used to evaluate the accuracy of greenhouse gas emission inventories. Many field studies have identified underestimates in the amount of CH₄ emitted from onshore oil and gas basin operations: production, gathering, processing, and transport (2–5). These underestimates can be large with some basins emitting multiples of the amount reported by official inventories (6–11). Much of this gap between observations and inventories can be explained by the presence of anomalously high emissions from a small number of sites termed superemitters (2, 11–14). CO₂ emissions from oil and gas basins, unlike CH₄, have not been extensively evaluated with field observations. We expect these emissions to be relatively well known since they should track with reported data on fuel use or equipment. Still, further investigation may be warranted since CO₂ is important to the overall climate budget; CO₂ often contributes to over half of basin greenhouse gas emissions (15, 16).

The ratio of emissions to production is a useful metric to compare climate impacts across basins, but the choice of metric can be misleading. Previous work has contextualized CH₄ emissions as natural gas loss rates, thereby attributing the losses entirely to the natural gas supply chain (4, 7, 9–10, 11–27). Yet, this accounting method inadvertently downplays the role of oil production in fugitive CH₄ emissions (28), especially in fields focused on oil and consequently less inclined to carefully manage recovery of associated gas. Attribution of production-related CO₂ and CH₄ emissions to both oil and gas is necessary for more accurate accounting of the origin of production-related greenhouse gas emissions and thus more informed mitigation choices. This issue of “coproduction” is addressed in the life cycle analysis (LCA) community with a set of codified methods for dividing impacts between products. We demonstrate an approach that addresses the coproduction issue with field measurement studies focused here on the US Gulf of Mexico (GOM).

Significance

Decisions on future energy production in the US Gulf of Mexico depend on climate impact assessments. We present an approach to calculate the carbon intensity of oil and gas production in the Gulf of Mexico using atmospheric observations of carbon dioxide and methane. We find that excess methane is emitted compared to government inventories. Platforms in shallow water have notably poor climate performance compared to either deep water or typical global oil production. Targeted shallow water mitigation measures for current or future production would have substantial climate benefits. The approach outlined here, including the use of observations of both greenhouse gases and attribution to both fossil products, could be widely applied to assess climate impacts of different production basins.

Author contributions: A.M.G.N. and E.A.K. designed research; A.M.G.N., E.A.K., Y.C., A.R.B., M.L.S., G.P., A.K.A., S.S., D.Z.-A., C.H., and Á.F.A.-C. performed research; A.M.G.N., Y.C., M.L.S., and A.R.B. analyzed data; and A.M.G.N., E.A.K., Y.C., and A.R.B. wrote the paper.

The authors declare no competing interest.

This article is a PNAS Direct Submission. J.A.d.G. is a guest editor invited by the Editorial Board.

Copyright © 2023 the Author(s). Published by PNAS. This open access article is distributed under [Creative Commons Attribution License 4.0 \(CC BY\)](https://creativecommons.org/licenses/by/4.0/).

¹To whom correspondence may be addressed. Email: agorchov@umich.edu or eakort@umich.edu.

This article contains supporting information online at <https://www.pnas.org/lookup/suppl/doi:10.1073/pnas.2215275120/-/DCSupplemental>.

Published April 3, 2023.

Oil and Gas Production in the GOM

The GOM is the largest offshore oil and gas basin in the United States and has been shown to emit more greenhouse gases than reported (23). Generally, platforms can be grouped into four broad categories that vary with size, supply chain role, and production rates. In shallow waters, production from small above water satellite facilities is gathered by a larger central hub facility, often a multiplatform complex, for processing. In shallow to mid-depth waters, medium platform installations serve both production and processing roles. In deep to ultradeep waters, large, generally newer facilities produce and process high volumes of oil and gas. Excess natural gas is typically expelled by direct cold venting in shallow waters and by flaring in deep waters. A series of field studies examining CH₄ emissions (23, 29–31) have found underestimates in shallow waters (23) and the presence of superemitting platforms, which tend to be central hub facilities (23, 31). The broader climate ramifications of these studies, which have included no evaluation of CO₂, have thus far remained unexplored.

A better understanding of GOM greenhouse gas emissions can inform mitigation and is particularly pertinent at this moment in influencing future production. Reductions in CO₂ and CH₄ emissions are required to lessen the future severity of climate change (32, 33). Potential sites for mitigation in the GOM have already been described (23, 31), but their impact on basin emissions is not well understood. Furthermore, expanded development of the GOM legally depends in part on the climate impacts of production. This is highlighted by a 2022 court ruling (34) that halted the sale of 1.7 million acres of leases received for auction (35) in federal shallow and deep waters. The court identified missing variables in a market simulation of life cycle greenhouse emissions from the global energy sector that compared a scenario with and a scenario without the GOM lease sale (34). The results of this simulation depend on the carbon intensity of GOM oil compared to oil produced from other locations (34). Further complexity is caused by the fact that oil is traded on international markets, and the impact of greater or lesser production in one location (like the GOM) could have effects on crude oil output in a variety of global regions with disparate marginal carbon intensities (36). While the Inflation Reduction Act of 2022 has mandated that the lease sale be reinstated (37, 38), there are up to 10 new lease sales proposed for the GOM between 2023 and 2028 (39, 40). To our knowledge, the official GOM CI has not integrated recent field measurements, and an update now would be timely given plans for further production and the resulting need for climate impact assessments.

Determining CI of Oil and Gas Production Using Observations

We study the climate impacts of current GOM production through a metric termed CI measured in grams of CO₂e of greenhouse gas emissions per megajoule of energy produced. A lower CI reflects a fuel with lower climate impacts per unit of energy delivered. The CI has become an increasingly important metric for fossil fuel producers and is of great interest in determining optimal investment by companies under carbon taxation or carbon emission limits. We argue that CI, instead of raw methane loss rates, is a more appropriate way to contextualize emissions from production operations as it allows for the inclusion of CO₂ emissions and allocation of emissions to both oil and gas. For this reason, it also allows a more accurate comparison of fields with different types of emission sources (e.g., heavy oil fields emit

significant amounts of CO₂ from combustion, while light oil fields may emit more CH₄).

The CI literature has poorly incorporated updates to total CH₄ emissions from field studies in production basins. This is because the CI literature tends to derive from the LCA world, which does not tend to perform actual field studies. Furthermore, the comparison of CI across studies is hindered by the diversity of ways it is constructed. In most cases, the CI is either a) computed by operators using proprietary data on field operations or b) estimated with engineering models that use properties of the operations to estimate likely emissions. Most academic studies use emission factors or engineering models (15, 16, 41–46), but a few have incorporated information from in situ observations to varying extents (5, 16, 46). Estimating the CI from aggregate top-down quantifications of CH₄ is possible (5) but has not been done in most studies as they are focused on granular constructs of CI. The CI is further complicated by different choices for numerators and denominators as some studies estimate the CI for only oil (15, 44), gas (45), or CH₄ (5).

This study differs in that we estimate the CI using direct field observations of plumes of CO₂ and CH₄ emitted from facilities. Here, the CI reflects total CO₂ and CH₄ emissions released from oil and gas production operations normalized by the energy content of the produced oil and gas. This CI does not include downstream emissions: refineries, transmission and storage, distribution, and end use. Nitrous oxide (N₂O) oil and gas emissions are comparatively small and not included in this study. To find total CO₂ and CH₄, we evaluate and update current emission inventories with atmospheric observations. We use facility-level gas flux estimates of CH₄, CO₂, and nitrogen oxides (NO_x = NO+NO₂), which are derived from airborne measurements collected in August 2020 as a part of the Flaring and Fossil Fuels: Uncovering Emissions and Losses (F³UEL) project (Fig. 1). Our CH₄ data are supplemented with additional field-based quantifications reported by all current studies for this domain (23, 29, 31) (Fig. 1), spanning all four categories of platforms (Fig. 2).

Observational Findings

We evaluate the most recent official inventories in federal and state waters. For federal waters, we compare with the US Bureau of Ocean Energy Management 2017 Gulfwide Offshore Activities Data System (GOADS) (47), which is used by the Environmental Protection Agency Greenhouse Gas Inventory (GHGI) (48). We modify the GOADS for 2021 by only including platforms with 2021 production. For state waters, the GHGI estimates emissions by using production-based emission factors created using BOEM's inventory. This includes CH₄, but does not encompass most CO₂ emissions, and is only reported in aggregate. We rescale the GHGI CH₄ by multiplying their emission factors by production for all platforms in state waters, which increases emissions (*SI Appendix, Table S1*). This is likely explained by our wider domain, which includes wetlands. To this point, *SI Appendix, Table S1* shows that the wetland contribution to production drives the majority of the production difference. State water CO₂ is estimated for central hubs using a ratio of emissions to production calculated from the GOADS inventory (for more details, see the *Materials and Methods* section, Calculation of CI).

Inventory emissions of CO₂ are generally consistent with observations from our aircraft survey, suggesting that combustion is well represented in the federal inventory. While there is considerable site-to-site variability, the inventory correlates with observations (Fig. 3, *Left* and Pearson coefficient of 0.73). For our sampled sites, total reported emissions of 144 t CO₂/h are in agreement with the

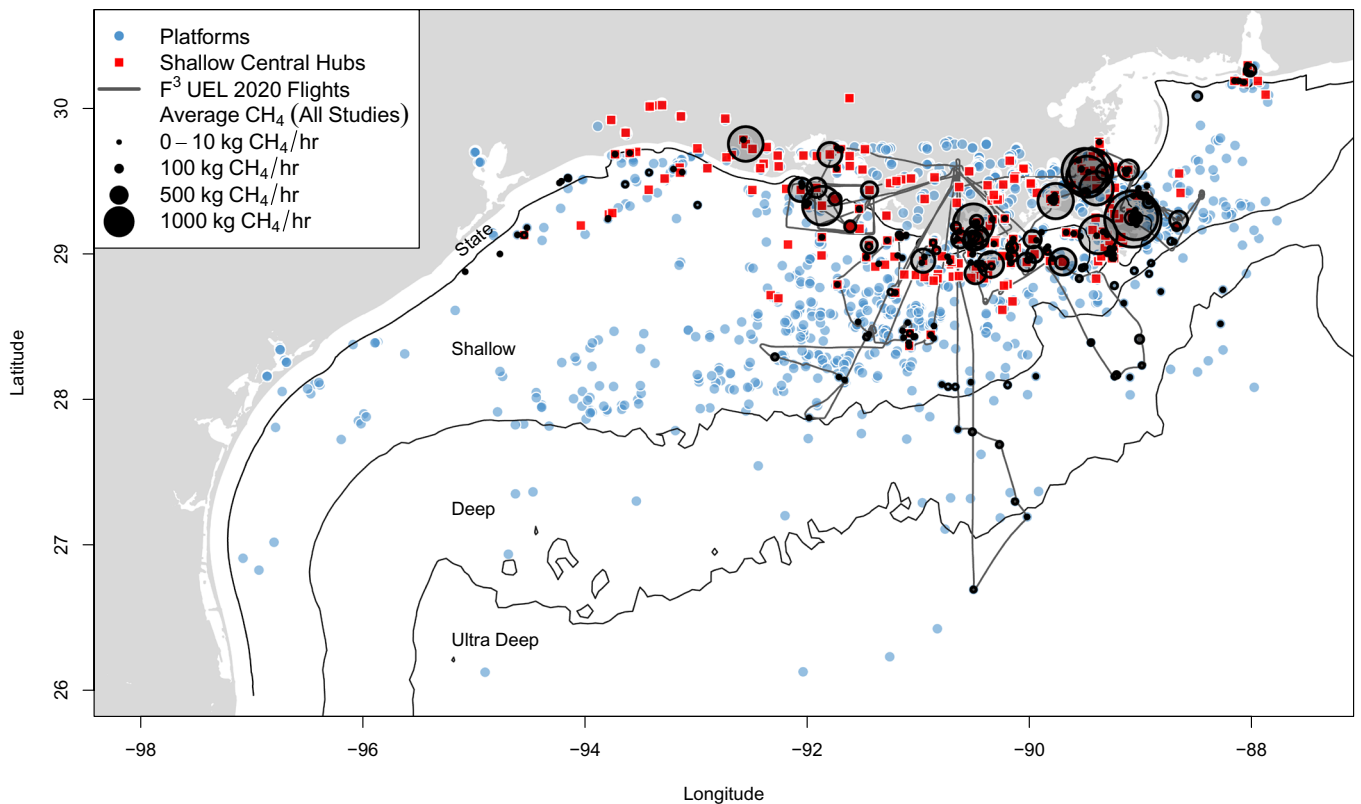


Fig. 1. Map of all platforms in the GOM and all samples used in this study. We show the flight tracks of the 2020 F³UEL campaign (black line) and the average of all existing CH₄ emission estimates from current field studies (black circles). Both central hub facilities (red squares) and other platforms (blue circles) are mapped out. The divisions between shallow (<200 m), deep (~200 to 1,520 m), and ultra-deep (>1,520 m) waters and between federal and state waters (three or nine nautical miles depending on the state) are shown. We observe the highest facility emission rates in shallow waters, especially at central hub facilities.

corresponding airborne total of 168 t CO₂/h [142 to 194, 95% confidence interval]. This result is supported by a similar evaluation of NO_x, another gas produced by combustion. While we find the inventory total of 418 kg NO_x/h is greater than the airborne total of 322 kg NO_x/h [283 to 360, 95% confidence interval], the inventory generally correlates with observations (Fig. 3, *Middle* and Pearson coefficient of 0.72). High rates of combustion in deep waters primarily drive these comparisons. Deep waters are expected

to be important to the budget of CO₂, representing 60% of federal inventory GOM platform emissions (47).

In contrast, CH₄ emissions are underestimated by inventories. At the site level, the inventory does not correlate with observations and underpredicts high-emitting sites, especially a number of central hubs (Fig. 3, *Right* and Pearson coefficient of 0.2). It is possible for short-duration measurements to sample rare high-emission events or miss important intermittent emissions, which can skew

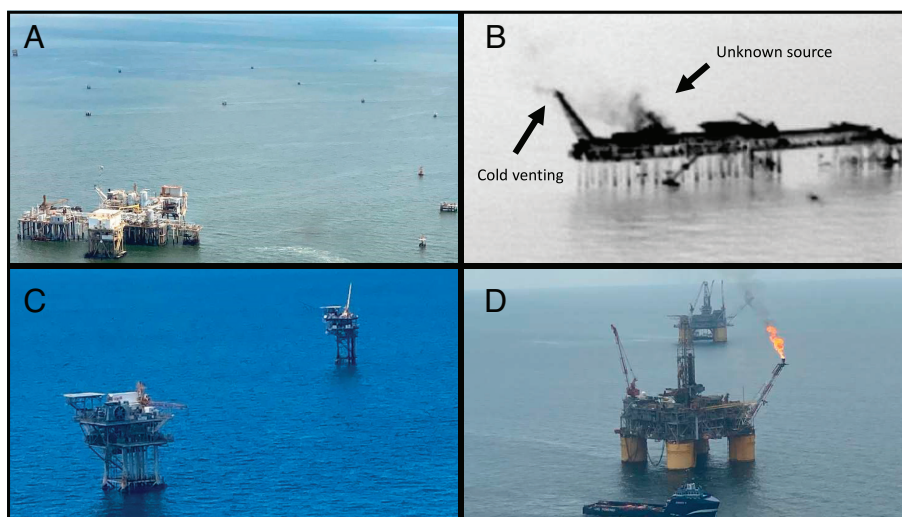


Fig. 2. Images taken of offshore facilities. (A) Small satellite facilities around a central hub facility. (B) Forward-looking infrared (FLIR) camera imagery of hydrocarbon emissions from a central hub facility. Two sources are identified: cold venting and an unknown piece of equipment. (C) Other shallow water facilities. (D) Deep water facilities with flaring.

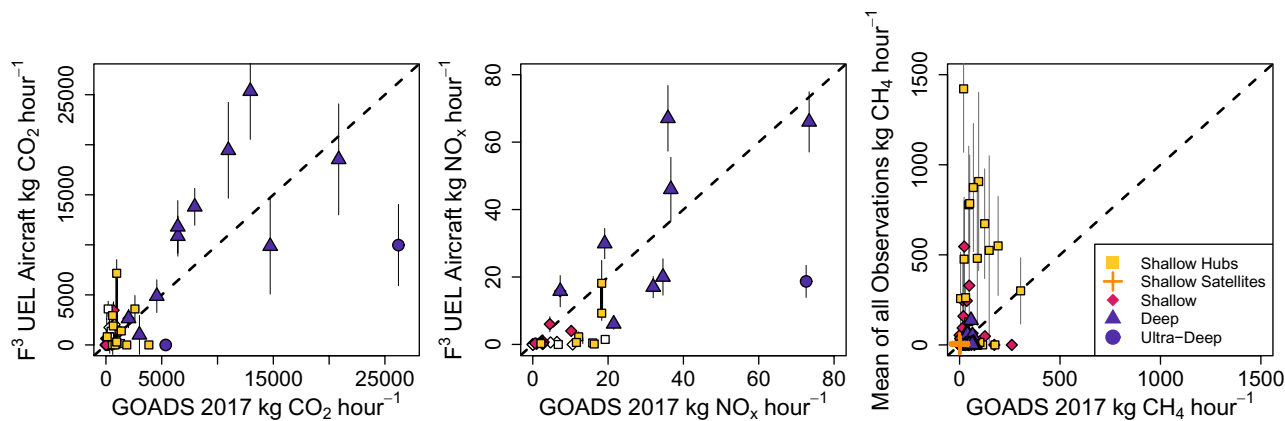


Fig. 3. Comparison of platform-level emissions in federal waters between observations (Y axis) to BOEM GOADS inventory (X axis). Facilities are categorized by the broad platform category (colored points) and shown as white if oil and gas production was zero during sampling. Combustion emissions of CO₂ (Left) and NO_x (Middle) are shown for daily fluxes calculated in this study from the F³UJEL airborne measurements. Error bars for CO₂ and NO_x represent the flux SD. CH₄ emissions (Right) are shown for the average flux across multiple days of observation from the F³UJEL survey in this study and all previous field surveys: Yacovitch et al. (2020) (29), Gorchoy Negron et al. (2020) (23), and Ayasse et al. (2022) (31). Error bars for CH₄ represent the SE calculated from the SD of the flux across days and number of days sampled.

interpretation (30). These high-emitting sites represent averages of multiple days of sampling, suggesting there is a pattern of sustained emissions (*SI Appendix, Fig. S1*). Note that there is no bias introduced to the range of estimated emissions with repeat visits (*SI Appendix, Fig. S2*). While this study does not resolve site-level intermittency, the distribution of emissions from central hubs is underestimated (*SI Appendix, Fig. S3*), even when accounting for intermittent hourly emissions implied by the inventory (*SI Appendix, Figs. S4–S6*). For a detailed discussion on reconciling intermittency, please see *SI Appendix, Appendix S1*.

To understand the implications of this, we create an observationally informed update to basin-wide CH₄ emissions. We resample all available facility-level atmospheric observations for each platform category using three separate approaches: resampling absolute flux rates, resampling gas loss rates, and resampling joules of oil and gas loss rates (*Materials and Methods*). We find comparable total CH₄ emissions regardless of the statistical method (*SI Appendix, Table S2*). This approach assumes that our sample set of platforms is representative of the population. To test this, we apply our resampling method using the inventory emission rates and find agreement with the original inventory (*SI Appendix, Figs. S7 and S8*).

Fig. 4 shows that updated CH₄ emissions are higher in both federal and state waters compared to the inventory approaches. Mean emissions are 3.0 and 13 times the federal and state water inventories. Total 2021 emissions are substantial [0.60 Tg/y (0.41 to 0.81, 95% confidence interval)]; they are greater than aircraft-based estimates found in the northeast Marcellus, PA [0.13 Tg/y (18)] and Bakken, ND [0.25 Tg/y (21)], and comparable to the Eagle Ford, TX [0.73 Tg/y (21)]. For the years corresponding to the most recent inventories, we find that emissions are even higher, and the underestimate by inventories is wider than in 2021 (*SI Appendix, Fig. S7 and Table S2*).

Our estimate of state water CH₄ is conservative since we limit our analysis to central hub platforms where we have sufficient observations to comment. This excludes potential emissions from ~1,700 state water satellite facilities, pipeline leaks, and multiple installations in Texas state waters that are not consistent with the central hub–satellite facility design. Although we anticipate these sources to be small in comparison to central hubs, they could be important. Ayasse et al. (2022) (31) have reported multiple instances of high emissions from satellite facilities, but we do not know the frequency of such events. Two samples from actively producing Texas sites (29) show relatively low emissions, but there

is at least one report of a large undetermined CH₄ leak from an orphaned platform (49). The issue of orphaned and abandoned wells, common in shallow waters, is beyond the scope of this paper.

Subsea leaks do occur but are not considered in this study. Ayasse et al. (2022) (31) identified multiple instances of CH₄ emissions from ephemeral leaks at subsea pipelines in shallow state waters. We do not know the frequency of these events and cannot comment on their aggregate emissions. It is conceivable that leaks occur at subsea infrastructure in deep waters. But here, moderate size leaks are unlikely to reach the surface before the CH₄ is dissolved (50).

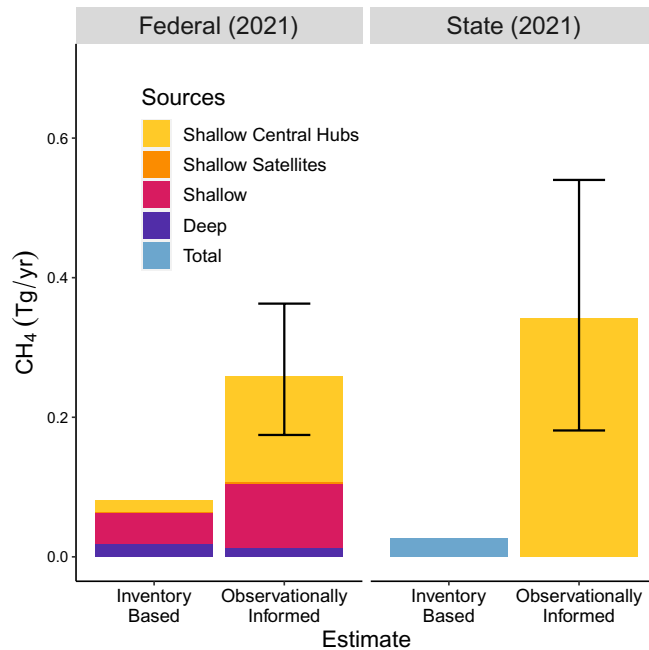


Fig. 4. Total CH₄ emissions for the GOM from inventories and observations for federal waters (Left) and state waters (Right). Observationally informed emissions are shown for the resampling of absolute flux rates (resampling approach A), with a mean and 95% confidence interval. The inventory estimates represent values adjusted for the year 2021. These were calculated from the 2017 GOADS for federal waters and from 2019 values reported in the 2021 GHGI for state waters. See *SI Appendix, Fig. S7* for a comparison made for years corresponding to the inventories. State water emissions are estimated only for central hubs because (a) the hub–satellite system dominates state water infrastructure and likely drives most emissions, and (b) our data are most complete for central hubs.

Explanation for High Methane Emissions

Platforms in shallow waters, especially central hubs, are most responsible for the gap in reported CH₄ emissions (Fig. 4). The satellite–central hub system dominates state waters but is a relatively small part of federal waters. Yet, the small number of underestimated high-emitting facilities in federal waters is responsible for at least 50% of federal water emissions (*SI Appendix, Fig. S8*).

Some central hub facilities have high loss rates because they have high emissions compared to moderate production (*SI Appendix, Fig. S9*) (see *SI Appendix, Appendix S2* for loss rate calculations) (23, 31). This is reminiscent of the onshore phenomenon of CH₄ emitted disproportionately from marginal wells (27). We observe that emissions of 100s–1000s of kg CH₄/hr are present regardless of central hub production rates (*SI Appendix, Fig. S10*). These facilities occupy multiple supply chain roles, which may explain why emissions are independent of production rate. Some of these sites may help transport gas from further offshore, but we are unsure as to how common this is and do not see any systematic differences in emission rates between sites with and without pipeline intersections from deeper waters.

High-emission events from these facilities are frequent and can be attributed to cold venting, emissions associated with tanks, and other pieces of equipment (31). Cold venting and unknown equipment sources are confirmed in our airborne survey for a number of high-emitting sites using infrared imagery collected by forward-looking infrared (FLIR) camera (Fig. 2*B*). Cold venting is expected to drive infrequent high-emission events but appears to be very persistent where present (31). While cold venting is expected to be metered for many of these facilities, it is possible for the venting to not be fully accounted due to the absence of metering or faulty meters. Another explanation is that operators may be underreporting venting as evidenced by a recent probe that found multiple platforms to be venting and flaring in excess of regulations for years; these were owned by a GOM oil company that had managed over 500 platforms (51). Other features associated with this category of platform may help explain why we observe high emissions. As they centralize production from multiple satellites, they could be handling volumes that at times differ widely from their optimal capacity. Maintenance and controls may be poorly implemented because they tend to be older and may have experienced bankruptcy on multiple

occasions. Emission rates vary between central hubs (*SI Appendix, Figs. S9 and S10*), but we are unable to identify any simple predictive indicators to explain why, including age of facility (*SI Appendix, Fig. S11*).

Observationally Determined CI

We estimate the CI of oil and gas production using our updated CH₄ emissions and the observationally verified inventory CO₂ estimate (*Materials and Methods*). CH₄ is a potent greenhouse gas with a comparatively short atmospheric lifetime, so the time horizon selected for conversion to a CO₂ equivalent (CO₂e) will determine its relevance. We report the CI for both a 100-y horizon, as is standard in government-issued inventories, and a 20-y horizon, to capture the importance of near-term warming (52) using global warming potentials of 28 and 84 g CO₂e/g CH₄ (1), respectively. We present findings for 2021 (Fig. 5 and *SI Appendix, Figs. S12 and S13 and Table S3*) and for the years corresponding to the most recent inventory available to show a direct comparison (*SI Appendix, Table S3*).

We report the CI mean and 95% confidence interval in g CO₂e/MJ over 100 y [20 y] in Fig. 5 and *SI Appendix, Fig. S12*. We find the full basin CI of 5.3 {13} [4.1 to 6.7 {10–17}] is 2.5 {3.4} times the inventory value of 2.1 {3.5}. The gap is wider over 20 y because CH₄ emissions are higher in the observations, making the CI more sensitive to near-term warming. Regional differences in the CI explain this basin-wide gap. A low CI of 1.1 {1.3} [–1.0 to 1.1 {1.2 to 1.4}] is found in deep waters, where combustion emissions dominate the climate impact and production is high, resulting in a large denominator of total MJ produced. In contrast, we observe particularly a high CI in shallow federal waters of 16 {49} (12 to 22 [32 to 68]) and state waters of 43 {118} [25 to 65 {65 to 184}] where CH₄ drives the majority of emissions and facilities have moderate production rates. The CI of state water production alone is close to the 100-y CI of full end use combustion of natural gas, ~50 to 55 g CO₂e/MJ (42, 43), and gasoline, ~70 g CO₂e/MJ (43), which should be the largest contributor to emissions. The state water CI is higher than the federal shallow water intensity because central hubs dominate production in state waters, while they are among other producing facilities in federal waters. *SI Appendix, Fig. S13* breaks these CIs down into separate contributions from oil and gas based on relative energy contents. This is an imperfect disaggregation

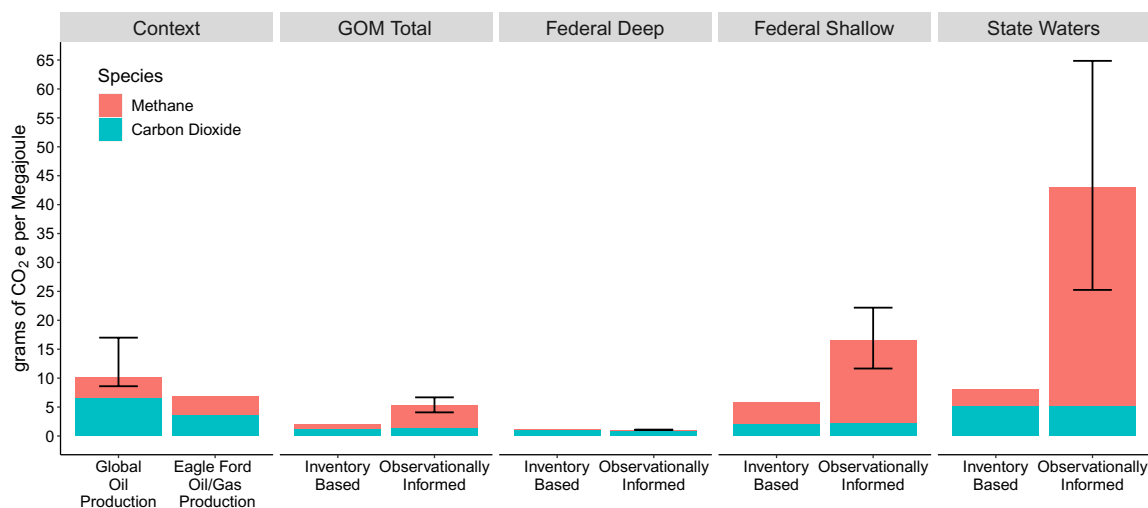


Fig. 5. The 100-y CI for 2021 in the US GOM basin compared to the literature. The observationally informed estimate draws from the resampling of absolute flux rates approach. Mean and 95% confidence intervals are shown. The literature value for global oil production is shown for Masnadi et al. (2018) (15) and for oil and gas production in Eagle Ford from Chen et al. (2019) (16). Observed shallow water CI is considerably higher than either deep water production or typical global oil production.

method but shows qualitatively that both oil and gas have substantial contributions to the GOM CI.

Comparison to other basins is difficult since our method to estimate the CI using direct observations has not been widely used. Given this, we compare with the CI of global oil production (from the well up to the refinery entrance), which is estimated by Masnadi et al. (2018) (15) using the Oil Production Greenhouse gas Emissions Estimator engineering model. Masnadi et al. only examine oil production and include different system boundaries that have additional emissions not covered by our study: drilling, field development, land disturbance, and embodied emissions from steel and cement. Therefore, the Masnadi et al. numbers will be of a somewhat different nature compared to our figures. We also compare with the CI of the nearby Eagle Ford, TX basin, estimated by Chen et al. (2019) (16). Chen et al. is perhaps the most similar existing approach to CI. While they use bottom-up emission inventories, they compare with oil and gas, include CO₂ and CH₄, and include revised CH₄ emissions for specific sources based on atmospheric observations.

The CI found for GOM production is within the range found in other regions. The GOM CI is slightly lower over 100 y {and comparable over 20 y} to the Eagle Ford, TX, CI of 6.8 g CO₂e/MJ {13} (16). The 100-y value is less than the global volume-weighted average CI of oil 10.3 g CO₂e/MJ (8.6 to 17) (15). However, over 20 y, the CI is on the lower bound of average oil production {17}. There is precedent for high regional variability, which we discuss here using 100-y horizons. Chen et al. (2019) (16) reported a range of 3.4 to 14 g CO₂e/MJ from production regions within the Eagle Ford, and Masnadi et al. (2018) (15) estimate that at least one oil field reached close to 50 g CO₂e/MJ. At the low end, Masnadi et al. found national averages in regions like Norway and Saudi Arabia to be in the range of 3 g CO₂e/MJ. However, our CI differs in that the majority of emissions come from CH₄ (74% over 100 y). High CIs due to CH₄ have been observed before; MacKay et al. (2021) (5) showed in Canadian oil and gas fields that CH₄ alone drove intensities over 30 g CO₂e/MJ.

Implications

This study demonstrates the importance of incorporating observation-based updates of total oil and gas CH₄ emissions into the CI for two reasons. First, this approach allocates CH₄ emissions to oil and gas production weighted by relative energy contents rather than allocating entirely to the natural gas supply chain. Given that production of oil is the primary economic driver in many of these basins, this accounting appears to better allocate emissions to the activity most responsible. Second, our results show that field-based updates to CH₄ emissions can have a large impact on CI, which are not incorporated in traditional CI evaluations. All CI evaluations should include CH₄, ideally from direct observations where available.

Our observationally determined production CI can provide the foundation for current and future assessments of the climate implications of production in the GOM and can be folded into full supply chain LCAs. We show that current CH₄ emissions in shallow waters are high and have caused an outsized climate impact in this region. If production continues or expands at high-emitting sites, the CI of Gulf fuels will continue to be elevated. Shallow water emissions will likely remain relevant despite declines in shallow water production and platforms since the year 2000. New drilling activity continues in shallow waters (*SI Appendix, Fig. S14*), including at high-emitting central hub facilities (*SI Appendix, Fig. S15*). Central hubs are a stable category of platform (53) and are projected to endure decommissioning trends (53). Prospective

lease sale maps place both deep and shallow waters up for auction (54). Mitigation efforts in shallow waters, especially targeting central hub facilities, have the opportunity to substantially reduce the climate impact of GOM production. This could be done through replacing venting with efficient flaring, refurbishing or repairing dilapidated equipment, and plug and abandonment.

Materials and Methods

Deployment and Sampling Strategy. In Fig. 1, we show aircraft flights that collected measurements from 52 offshore oil and gas platforms in the GOM during August 2020 as part of the Flaring & Fossil Fuels: Uncovering Emissions & Losses (F³UEL) project (<http://graham.umich.edu/f3uel>). Our goals were to study emissions of CH₄, CO₂, and NO_x, gather a representative sample of the very diverse GOM oil and gas system, and to collect extensive data from the highest sources of emissions. We sampled platforms in ultradeep, deep, shallow, and wetland regions from a variety of different infrastructure categories, under different production rates, and operated by different companies. For clarity, we consider wetland sites to belong to shallow waters.

We identified two types of high-emitting sites for extensive sampling. For CH₄, we prioritized sampling of shallow water central hub facilities, which are known to have intermittent high-emission events (23, 31). Therefore, we sampled facilities of different size categories and production rates, and we conducted repeat sampling several days apart to avoid resampling any rare multiday blowdown events. For NO_x, we targeted two sites in deep waters that correspond to NO₂ enhancements observed with the TROPOspheric Monitoring Instrument, which overlap with four platforms reported to emit high NO_x.

Instrumentation. Measurements were collected by Scientific Aviation (<https://www.scientificaviation.com/>) with a Mooney aircraft modified with under the wing inlets for collection of meteorological data and trace gas concentrations. We gathered CH₄, CO₂, H₂O with a Picarro G2401 (<https://www.picarro.com/>), NO with EcoPhysics 88 NOe (<https://www.ecophysics-us.com/>), NO₂ with a Teledyne T5000U (<https://www.teledyne-api.com/>), and O₃ with 2B Technologies (<https://twobtech.com/index.html>). Global Positioning System antennae (Hemisphere Precision GPS) are used to collect location, altitude, heading, and speed. The Vaisala HMP60 probe (<https://www.vaisala.com/en>) recorded temperature and humidity. FLIR camera imagery was collected to identify sources of hydrocarbons. Horizontal winds are estimated according to Conley et al. (2014) (55).

Quantification of Facility Emissions. We estimate facility-level emission rates following Conley et al. (2017) (56). In this approach, the aircraft flies in concentric rings around a facility from the lowest altitude feasible up until the maximum altitude the plume is present, creating a cylindrical flight pattern. The emission rate is estimated from the sum of the flux divergence, calculated for each altitudinal path by Gauss's Theorem, and the change in mass over time in the following equation:

$$Q_c = \left\langle \frac{\partial m}{\partial t} \right\rangle + \int_0^{z_{\max}} \oint \dot{c}' u_h \cdot n \, dldz$$

Here, Q_c is the sum of sources and sinks of the species within the volume, $\left\langle \frac{\partial m}{\partial t} \right\rangle$ is the average change in mass over time, z is the altitude of the flight path from the bottom ring to the top ring, \dot{c}' is the perturbation concentration relative to the mean concentration of a given loop, and n is an outward facing unit vector.

The method requires a sufficient level of vertical mixing to disperse the plume so that it is above the lowest altitude the aircraft can fly and dispersed enough to be sampled by the aircraft. However, this method does not require the plume to be well mixed throughout the vertical extent of the mixed layer. This is possible since the aircraft directly measures the vertical extent of the plume and requires no vertical extent assumptions to be made. Therefore, the aircraft must fly far enough away from the source for sufficient dispersion but close enough to detect a signal. The largest source of uncertainty is expected to be whether the plume is captured by the lowest loop. In one sense, this is easier over the ocean where the lowest loop can be relatively close to the surface (~50 m) but difficult under limited mixing conditions sometimes found within the marine boundary layer. We sampled in August with warm waters leading to thermal gradients that favor sufficient mixing.

We extrapolate from the lowest loop to the surface based on an estimated convective velocity (derived from the SD of wind speeds and boundary layer height). The sensitivity of the flux to this extrapolation is minimized by a sampling distance that is far enough away for sufficient vertical lofting to have decreased the vertical gradient in the flux divergence.

Flux error is estimated following Conley et al. (2017). This error represents a) the variability introduced by turbulence for legs along the same altitude and b) the time rate of change. To estimate the former error, we group legs into bins, calculate the SD of the horizontal fluxes within a bin, and propagate the uncertainties by quadrature. The latter error is the least squares fit between CH₄ density, time, and altitude. The two errors are combined by quadrature.

The application of this method to estimate NO₂ is complicated by sampling gaps in continuous data for calibrations. We report emission rates for the sites where we have confidence that we captured the majority of the plume associated with combustion. To this end, we compare the CO₂ flux estimated using the full continuous data to an alternative CO₂ flux that is estimated only using data that coincide with available NO₂ measurements. We assign confidence to sites where the mean and SD from either flux scenario include the mean of the other. This same approach has successfully been applied to facility emissions of N₂O (57). Most sites satisfy this stipulation and those that did not are removed from our analysis.

Estimation of Basin-Wide CH₄ Using Four Field Studies. We incorporate all existing facility-level samples collected in the GOM to estimate CH₄: Yacovitch et al. (2020) (29), Gorchov Negron et al. (2020) (23), and Ayasse et al. (2022) (31). Together, with this study, these studies sampled in total 143 unique federal water platforms and 91 unique state water central hubs. Data were collected across 3 y of sampling that include all seasons, consist of airborne and ship-based measurements, and involve three independent methods of quantification. Certain considerations are made to create this dataset. For sites taken from Yacovitch et al., we only use plumes that Yacovitch et al. confidently linked to a facility. Sites taken from Ayasse et al. include nondetected sites, which we label as zero emission sites for our analysis. We gathered these from Ayasse et al. and then added more that we determined to be within areas they sampled.

It can be difficult to use oil and gas CH₄ emissions at the facility level to comment on total CH₄ emissions. Sampled sites can potentially have large variations in emissions of an order of magnitude that can deviate widely from the average, while unsampled sites may include superemitters. Site-level intermittency is difficult to estimate based on a handful of emission profile snapshots.

We construct our estimate of basin-wide emissions using stratified resampling of observations, which does not require us to resolve questions of intermittency. We expect that certain types of platforms will have similar emission profiles. Therefore, a sufficiently large random sample of facilities that have similar behavior should be representative of the average of the full population of that type of facility. Grouping central hub platforms is particularly important since they show the largest intermittent emission deviations. While we do not have a complete time series of a given central hub, our sample of central hubs is substantial, encompassing 35 of 93 unique facilities in federal waters and 91 of 160 unique facilities in state waters, many of which had repeat visits. With enough spatial samples, we should account for temporal variability because of the inherent randomness in event occurrences, which means that as we sample in space we are sampling in time. This is somewhat similar to the idea behind the Birkhoff Ergodic Theorem (58), which posits that for a dynamical system where most points eventually revisit the set, the time average of one point will be the same of the average over the full space. For a more detailed discussion on reconciling site-level intermittency, see *SI Appendix, Appendix S1*.

We classify platforms into four broad categories: satellite facilities that support production for central hubs, central hubs, other shallow water facilities that have collocated production and processing, and deep water facilities that include a couple of ultradeep installations. *SI Appendix, Fig. S9* compares these categories across all field campaigns, showing that the distribution of absolute emission rates is similar within each category. The difference between mean emissions from emitting facilities appears reduced when emissions are normalized by production. This supports the use of these categories for stratified sampling. Furthermore, we explore what characteristics may be predictive of emissions from central hub facilities but find no correlation (*SI Appendix, Fig. S11*).

Total emissions are estimated separately for GOM federal waters and GOM state waters using three methods. We separate our samples by federal and state water jurisdictions to account for any differences between regulations or monitoring. This is supported by Ayasse et al. (2022) (31), who report that state water loss rates are higher than those in shallow federal waters. Before we assign an emission rate to a platform, we determine whether the facility is active. We use production to indicate the active status of a platform. We treat platforms with zero oil and gas production as a proxy for inactive facilities and assign zero emissions. An emission rate is assigned to every platform in the population based on a directly observed value drawn from the corresponding platform category within the dataset of sampled sites. This is done using absolute emission rates in terms of kg CH₄ h⁻¹ (A), equivalent natural gas loss rates (B), or equivalent oil and gas joule loss rates (C). A mean and 95% confidence interval are generated from the sampling distribution of the total emissions estimated by 1,000 simulations.

For the absolute emission rate approach, the emission rate is assigned by randomly selecting a representative facility, randomly selecting one of possibly multiple days of observations at the site, and drawing a value from the normal distribution generated from the mean CH₄ flux and SD found in the field. This incorporates the flux error at the field survey level into our simulated distributions. For the two loss rate approaches, an emission rate is assigned by selecting the three representative platforms with the closest production rate to the platform under consideration, randomly selecting one of possibly multiple days of observations for each of the three sites, drawing three loss rates from the normal distribution generated from each of the three mean loss rates and SDs, and finally reporting the average of the three values. The reason we generate an average value from three loss rates instead of one value is to reduce the influence of outlier loss rates, which can bias the simulation if many facilities produce at rates close to an outlier. In practice, this approach mirrors a loss rate vs production curve but creates variability similar to observations and avoids the limitations of curve fitting that can lead to biases introduced by outliers. We cap values to absolute flux emissions no higher than those observed in the field. *SI Appendix, Fig. S16* illustrates how these three approaches generate a simulated distribution similar to observations.

The most recent official inventories are generated for 2017 in federal waters by the 2017 BOEM GOADS inventory and 2019 in state waters by the 2021 GHGI. Therefore, we make a series of two estimates. One for the time period directly corresponding to the inventory and another for 2021 to understand how emissions are behaving more recently. *SI Appendix, Table S2* reports our estimates for each of the three extrapolation approaches.

Calculation of CI. We estimate the CI by dividing greenhouse gas emissions by joules of energy produced. We convert oil and gas production to joules of energy (*SI Appendix, Appendix S2*). For CH₄, we use the updated CH₄ values calculated by the resampling approach A. We choose approach A because it usually agrees with the other methods, generally has wider confidence intervals, represents the simplest method, and makes the most intuitive sense. Emissions appear to track with facility type regardless of production rate.

For CO₂, we directly utilize the federal GOADS inventory because our observations suggest it correctly captures combustion emissions and it is a complete dataset. There is no complete CO₂ inventory for state waters, and too few observations are available to create an independent estimate. Therefore, we adapt the federal inventory for the state water system. We update the estimate of CO₂ emissions in state waters by rescaling total CO₂ from central hubs and satellites in federal waters by state water production. This assumes that state water CO₂ follows the same pattern of CO₂ emitted from the central hub-satellite system in federal waters. We think this assumption holds true as a) most state water facilities follow the central hub-satellite system and b) we do not see a different pattern of CO₂ emissions between observations of hubs in state vs federal waters. Our state water CI is conservative since it includes all production but assumes that emissions only come from central hub facilities.

Data, Materials, and Software Availability. Aircraft data from the 2020 GOM F³UCL survey is available at <https://doi.org/10.7302/1xjm-3v49> (59). *Datasets S1–S3* contain flux rates used in this study, which were collected from the 2020 GOM F³UCL survey and adapted from the Spring and Fall deployments from Ayasse et al. (2020), including nondetections, are reported with *SI Appendix*. See Ayasse et al. (2022) for

the most up to date version of fluxes used in their study. See Yacovitch et. al (2020) for flux rates taken from their study (29).

ACKNOWLEDGMENTS. We thank Paolo Wilczak for help with data collection. The F³UEL project was funded by the Alfred P. Sloan Foundation and supported by the Environmental Defense Fund, Scientific Aviation, and the University of Michigan (College of Engineering, Climate and Space Sciences and Engineering) and the Graham Sustainability Institute. Funding for the Global Airborne Observatory (GAO) flights and data analysis was supported by Carbon Mapper, the University of Arizona, and the numerous Carbon Mapper funders. GAO is managed by the Center

for Global Discovery and Conservation Science at the Arizona State University and is made possible from the support of private foundations and visionary individuals.

Author affiliations: ^aDepartment of Climate and Space Sciences and Engineering, University of Michigan, Ann Arbor, MI 48109; ^bDepartment of Energy Science and Engineering, Stanford University, Stanford, CA 94305; ^cScientific Aviation, Boulder, CO 80301; ^dArizona Institutes for Resilience, University of Arizona, Tucson, AZ 85719; ^eCarbon Mapper, Pasadena, CA 91105; ^fEnvironmental Defense Fund, Washington, DC 20009; ^gGerald R. Ford School of Public Policy, University of Michigan, Ann Arbor, MI 48109; and ^hDepartment Atmospheric and Oceanic Sciences, University of Wisconsin, Madison, WI 53706

1. IPCC, AR5 Climate Change 2013: The Physical Science Basis – IPCC (5 September 2022).
2. A. R. Brandt et al., Methane Leaks from North American natural gas systems. *Science* **343**, 733–735 (2014).
3. A. J. Marchese et al., Methane emissions from United States natural gas gathering and processing. *Environ. Sci. Technol.* **49**, 10718–10727 (2015).
4. R. A. Alvarez et al., Assessment of methane emissions from the U.S. oil and gas supply chain. *Science* **361**, 186–188 (2018).
5. K. Mackay et al., Methane emissions from upstream oil and gas production in Canada are underestimated. *Sci Rep.* **11**, 8041 (2021).
6. E. A. Kort et al., Four corners: The largest US methane anomaly viewed from space. *Geophys. Res. Lett.* **41**, 6898–6903 (2014).
7. G. Pétron et al., A new look at methane and nonmethane hydrocarbon emissions from oil and natural gas operations in the Colorado Denver-Julesburg Basin. *JGR Atmospheres* **119**, 6836–6852 (2014).
8. E. Chan et al., Eight-year estimates of methane emissions from oil and gas operations in Western Canada are nearly twice those reported in inventories. *Environ. Sci. Technol.* **54**, 14899–14909 (2020).
9. Y. Zhang et al., Quantifying methane emissions from the largest oil-producing basin in the United States from space. *Sci. Adv.* **6**, eaaz5120 (2020).
10. L. Shen et al., Unravelling a large methane emission discrepancy in Mexico using satellite observations. *Remote Sens. Environ.* **260**, 112461 (2021).
11. Y. Chen et al., Quantifying regional methane emissions in the New Mexico Permian basin with a comprehensive aerial survey. *Environ. Sci. Technol.* **56**, 4317–4323 (2022).
12. D. Zavala-Araiza et al., Reconciling divergent estimates of oil and gas methane emissions. *Proc. Natl. Acad. Sci. U.S.A.* **112**, 15597–15602 (2015).
13. A. R. Brandt, G. A. Heath, D. Cooley, Methane leaks from natural gas systems follow extreme distributions. *Environ. Sci. Technol.* **50**, 12512–12520 (2016).
14. D. R. Lyon et al., Aerial surveys of elevated hydrocarbon emissions from oil and gas production sites. *Environ. Sci. Technol.* **50**, 4877–4886 (2016).
15. M. S. Masnadi et al., Global carbon intensity of crude oil production. *Science* **361**, 851–853 (2018).
16. Q. Chen, J. B. Dunn, D. T. Allen, Aggregation and allocation of greenhouse gas emissions in oil and gas production: Implications for life-cycle greenhouse gas burdens. *ACS Sustainable Chem. Eng.* **7**, 17065–17073 (2019).
17. A. Karion et al., Aircraft-based estimate of total methane emissions from the Barnett Shale Region. *Environ. Sci. Technol.* **49**, 8124–8131 (2015).
18. J. Peischl et al., Quantifying atmospheric methane emissions from the Haynesville, Fayetteville, and northeastern Marcellus shale gas production regions. *J. Geophys. Res. Atmosph.* **120**, 2119–2139 (2015).
19. J. Peischl et al., Quantifying atmospheric methane emissions from oil and natural gas production in the Bakken shale region of North Dakota. *J. Geophys. Res. Atmosph.* **121**, 6101–6111 (2016).
20. M. R. Johnson, D. R. Tyner, S. Conley, S. Schwietzke, D. Zavala-Araiza, Comparisons of airborne measurements and inventory estimates of methane emissions in the alberta upstream oil and gas sector. *Environ. Sci. Technol.* **51**, 13008–13017 (2017).
21. J. Peischl et al., Quantifying methane and ethane emissions to the atmosphere from Central and Western U.S. oil and natural gas production regions. *J. Geophys. Res. Atmosph.* **123**, 7725–7740 (2018).
22. S. N. Riddick et al., Methane emissions from oil and gas platforms in the North Sea. *Atmosph. Chem. Phys.* **19**, 9787–9796 (2019).
23. A. M. Gorchov Negron, E. A. Kort, S. A. Conley, M. L. Smith, Airborne assessment of methane emissions from offshore platforms in the U.S. Gulf of Mexico. *Environ. Sci. Technol.* **54**, 5112–5120 (2020).
24. J. C. Lin et al., Declining methane emissions and steady, high leakage rates observed over multiple years in a western US oil/gas production basin. *Sci Rep.* **11**, 22291 (2021).
25. D. Zavala-Araiza et al., A tale of two regions: Methane emissions from oil and gas production in offshore/onshore Mexico. *Environ. Res. Lett.* **16**, 024019 (2021).
26. A. Foulds et al., Quantification and assessment of methane emissions from offshore oil and gas facilities on the Norwegian continental shelf. *Atmosph. Chem. Phys.* **22**, 4303–4322 (2022).
27. M. Omara et al., Methane emissions from US low production oil and natural gas well sites. *Nat. Commun.* **13**, 2085 (2022).
28. D. T. Allen, Q. Chen, J. B. Dunn, Consistent metrics needed for quantifying methane emissions from upstream oil and gas operations. *Environ. Sci. Technol. Lett.* **8**, 345–349 (2021).
29. T. I. Yacovitch, C. Daube, S. C. Herndon, Methane emissions from offshore oil and gas platforms in the Gulf of Mexico. *Environ. Sci. Technol.* **54**, 3530–3538 (2020).
30. Z. Chen et al., Reconciling methane emission measurements for offshore oil and gas platforms with detailed emission inventories: Accounting for emission intermittency. *ChemRxiv [Preprint]* (2022). <https://chemrxiv.org/engage/chemrxiv/article-details/628bdbc6cae1c5f5c148516> (Accessed 5 September 2022).
31. A. K. Ayasse et al., Methane remote sensing and emission quantification of offshore shallow water oil and gas platforms in the Gulf of Mexico. *Environ. Res. Lett.* **17**, 084039 (2022).
32. IPCC, AR6 climate change 2022: Mitigation of climate change—IPCC (5 September 2022).
33. I. B. Ocko et al., Acting rapidly to deploy readily available methane mitigation measures by sector can immediately slow global warming. *Environ. Res. Lett.* **16**, 054042 (2021).
34. Friends of the Earth et al., v Debra A. Haaland et al. 1:21-cv-02317-RC - Document 78 (United States District Court, District of Columbia, 2022). <https://int.nyt.com/data/documenttools/78-memorandum-opinion-1-27/b0903c94e57b0cb5/full.pdf>. Accessed 9 May 2022.
35. Bureau of Ocean Energy Management, Lease sale 257 statistics. (2021) <https://www.boem.gov/oil-gas-energy/leasing/regional-leasing/lease-sale-257>. Accessed 5 September 2022.
36. M. S. Masnadi et al., Carbon implications of marginal oils from market-derived demand shocks. *Nature* **599**, 80–84 (2021).
37. J. Stein, M. Joselow, R. Roubein, How the Inflation Reduction Act might affect you – and change the U.S. *The Washington Post*, 15 August 2022. <https://www.washingtonpost.com/us-policy/2022/07/28/manchin-schumer-climate-deal/>. Accessed 5 September 2022.
38. Inflation Reduction Act of 2022. H.R. 5376, 117th Congress <https://www.documentcloud.org/documents/22122279-inflation-reduction-act-of-2022>. Accessed 5 September 2022.
39. M. Gordon, US Interior proposes up to 11 offshore oil, gas lease sales in 2023–2028. <https://www.spglobal.com/commodityinsights/en/market-insights/latest-news/natural-gas/070122-us-interior-proposes-up-to-11-offshore-oil-gas-lease-sales-in-2023-2028>. Accessed 21 December 2022.
40. Bureau of Ocean Energy Management, National OCS Oil and Gas Leasing Program for 2023–2028. <https://www.boem.gov/oil-gas-energy/national-program/national-ocs-oil-and-gas-leasing-program-2023-2028>. Accessed 21 December 2022.
41. M. Jiang et al., Life cycle greenhouse gas emissions of Marcellus shale gas. *Environ. Res. Lett.* **6**, 034014 (2011).
42. A. Venkatesh, P. Jaramillo, W. M. Griffin, H. S. Matthews, Uncertainty in life cycle greenhouse gas emissions from United States natural gas end-uses and its effects on policy. *Environ. Sci. Technol.* **45**, 8182–8189 (2011).
43. A. Burnham et al., Life-cycle greenhouse gas emissions of shale gas, natural gas, coal, and petroleum. *Environ. Sci. Technol.* **46**, 619–627 (2012).
44. M. M. Rahman, C. Canter, A. Kumar, Greenhouse gas emissions from recovery of various North American conventional crudes. *Energy* **74**, 607–617 (2014).
45. Y. Gan et al., Carbon footprint of global natural gas supplies to China. *Nat. Commun.* **11**, 824 (2020).
46. W. Contreras et al., Life cycle greenhouse gas emissions of crude oil and natural gas from the Delaware Basin. *J. Cleaner Production* **328**, 129530 (2021).
47. Bureau of Ocean Energy Management, OCS Emissions Inventories. <https://www.boem.gov/environment/environmental-studies/ocs-emissions-inventories>. Accessed 5 September 2022.
48. Environmental Protection Agency, Inventory of U.S. Greenhouse Gas Emissions and Sinks: 1990–2020 EPA 430-R-22-003. <https://www.epa.gov/ghgemissions/draft-inventory-us-greenhouse-gas-emissions-and-sinks-1990-2020>. Accessed 5 September 2022.
49. R. Gold, An oil well off padre island leaked for months before it was plugged. *Texas Monthly*, 29 June 2022. <https://www.texasmonthly.com/news-politics/oil-well-padre-island-leaked-months-before-plugged/>. Accessed 6 September 2022.
50. Ø. Johansen, H. Rye, C. Cooper, DeepSpill—Field study of a simulated oil and gas blowout in deep water. *Spill Sci. Technol. Bull.* **8**, 433–443 (2003).
51. E. Nilsen, Federal watchdog found oil and gas company likely defrauded government amid agency missteps. *CNN*, 6 September 2022. <https://www.cnn.com/2022/06/15/politics/interior-watchdog-report-fraud-methane-venting-climate/index.html>. Accessed 15 June 2022.
52. I. B. Ocko et al., Unmask temporal trade-offs in climate policy debates. *Science* **356**, 492–493 (2017).
53. M. J. Kaiser, S. Narra, A hybrid scenario-based decommissioning forecast for the shallow water U.S. Gulf of Mexico, 2018–2038. *Energy* **163**, 1150–1177 (2018).
54. Bureau of Ocean Energy Management, Active leases and bids received map. https://www.boem.gov/sites/default/files/documents/oil-gas-energy/leasing/sale-257-active-leases-map_1.pdf. Accessed 9 May 2022.
55. S. A. Conley, I. C. Faloon, D. H. Lenschow, A. Karion, C. Sweeney, A low-cost system for measuring horizontal winds from single-engine aircraft. *J. Atmosph. Oceanic Technol.* **31**, 1312–1320 (2014).
56. S. Conley et al., Application of Gauss's theorem to quantify localized surface emissions from airborne measurements of wind and trace gases. *Atmos. Meas. Tech.* **10**, 3345–3358 (2017).
57. A. Gvakharia, E. A. Kort, M. L. Smith, S. Conley, Evaluating cropland N₂O emissions and fertilizer plant greenhouse gas emissions with airborne observations. *J. Geophys. Res. Atmosph.* **125**, e2020JD032815 (2020).
58. G. D. Birkhoff, Proof of the ergodic theorem. *Proc. Natl. Acad. Sci. U.S.A.* **17**, 656–660 (1931).
59. E. A. Kort et al., "Aircraft Data (2020) for Flaring & Fossil Fuels: Uncovering Emissions & Losses (F3UEL) [Data set]." University of Michigan—Deep Blue Data. <https://doi.org/10.7302/1xjm-3v49>. Deposited 4 July 2022.